Biophysical Chemistry 40 (1991) 169–179
Elsevier Science Publishers B.V., Amsterdam

BIOCHE 01566

Persistence length and bending dynamics of DNA from electrooptical measurements at high salt concentrations

Dietmar Porschke

Max-Planck-Institut für biophysikalische Chemie, 34 Göttingen, Germany

Received 3 September 1990
Revised manuscript received 5 December 1990
Accepted 28 December 1990

Bending dynamics; Dichroism decay; Electrooptics; Persistence length; Rotational diffusion; (DNA)

A new electrooptical apparatus has been used to characterize the dichroism decay time constants for a collection of nine blunt-ended DNA restriction fragments in the range of chain lengths from 41 to 256 base-pairs at physiological salt concentrations. The experimental data show an increase of rotational diffusion coefficients, when the monovalent salt concentration is increased from a few mM, used previously for standard electrooptical experiments, to the range of salt concentrations around 100 mM. The presence or absence of 10 mM Mg^{2+} in a buffer with 100 mM NaCl does not induce any large change of the rotational diffusion. Bending of double helices is reflected by a fast component in the dichroism decay for fragments ≥ 90 bp; the time constant of the first bending mode is 7–9% relative to the time constant of overall rotational diffusion for fragments with 90 to 179 bp at the temperatures 2, 10 and 20 °C. Interpretation of the overall rotational diffusion time constants by different models on the hydrodynamics of flexible polymer chains leads to diverging values of the persistence length. The most accurate description is expected from a combination of the rotational diffusion coefficient for rigid rods given by Tirado and Garcia de la Torre (J. Chem. Phys. 73 (1980) 1986) with correction factors derived from Monte Carlo simulations (P.J. Hagerman and B.H. Zimm, Biopolymers 20 (1981) 1481). This model leads to 'average' values of the persistence length of 440, 400 and 380 Å at the temperatures 20, 10 and 2 °C, respectively (in 110 mM Na^+ and 10 mM Mg^{2+}, pH 7.0); the hydrodynamic radius of the helix is approx. 12.5 Å. The persistence lengths measured at various monovalent salt concentrations can be represented as a linear function of the reciprocal square root of the ionic strength. The rotational time constants measured for individual fragments at physiological salt show clearly larger deviations from the model average than corresponding time constants measured previously at low salt; 'apparent' persistence lengths of individual fragments as well as their temperature dependence show strong variations. Thus, it is hardly possible to define a 'standard' persistence length for mixed sequences — even though the sequences used in the present investigation do not show clear deviations from standard gel mobilities. These data indicate that formation of individual, sequence-directed structures of DNA fragments is favoured under physiological salt conditions.

1. Introduction

The stiffness of DNA double helices has been analyzed by many authors and by a large number of different techniques [1–16]. In spite of these efforts, a general agreement on the magnitude of the DNA stiffness has not been established. The exact numerical value of the DNA stiffness is not only a problem of academic interest but also has important implications with respect to the biological function of DNA. In biological systems DNA is usually found in a relatively compact state with a high degree of bending. Thus, the free energy of DNA bending, which is directly related to the DNA stiffness described by the persistence length, can be extremely large.

The majority of authors have published values of the persistence length close to 500 Å, while a minority have given lower values in the range around 300–350 Å. One problem may be that most experimental investigations have been performed on sonicated DNA samples, which are not

0301-4622/91/$03.50

really well defined. Another problem apparently results from the widely different ion concentrations used in the various investigations. Finally, as shown below, the model used for evaluation can lead to a rather large difference in the resulting persistence length.

Among the various physical methods used for measurements of persistence lengths, the most attractive ones are those which are based on the evaluation of rotational diffusion. This is due to the dependence of the rotational diffusion coefficients on the third power of the effective hydrodynamic dimensions. Electrooptical procedures [17,18] combine this very useful feature with the further advantages of a high sensitivity at a low demand on DNA quantities. Electrooptical measurements with DNA restriction fragments provide most accurate values of the persistence length. However, a serious problem associated with electrooptical measurements used to be the limitation to rather low ion concentrations. In the present investigation the rotational diffusion of DNA restriction fragments is characterized by a new electrooptical procedure, which has been developed for measurements at high salt concentrations [19]. The new experimental data demonstrate that the persistence length at physiological salt concentration is lower than that found previously from electrooptical measurements at low salt concentrations. The present measurements also show that it is hardly possible to define a standard persistence length because of rather strong variations found for individual DNA fragments.

2. Materials and methods

The DNA fragments were obtained from the plasmids pVH27 and pWH923, which were supplied by W. Hillen. Digestion of the plasmid DNAs with *Hae*III restriction endonuclease under standard conditions provided a mixture of blunt-ended fragments including helices with 43, 69, 84, 179 and 256 bp, which were separated by high-performance liquid chromatography (HPLC) on Nucleogen (Macherey-Nagel, Düren, Germany) according to the procedure of Colpan and Riesner [20]. Further digestion of the 179 and 256 bp fragments with *Mvn*I restriction endonuclease provided fragments with 41/138 and 90/166 bp, respectively, which were again separated by the HPLC procedure given above. The fragments were dialysed extensively: first against 1 M NaCl, 1 mM sodium cacodylate pH 7.0, 0.2 mM EDTA and then against 1 mM NaCl, 1 mM sodium cacodylate pH 7.0, 0.2 mM EDTA (buffer E) or 1 mM NaCl, 1 mM sodium cacodylate pH 7.0, 0.2 mM $MgCl_2$ (buffer M). The final salt concentrations used for the measurements were made up by addition of the required components. Buffer A contained 100 mM NaCl, 1 mM sodium cacodylate and 0.2 mM EDTA; buffer B: 100 mM $NaClO_4$, 1 mM sodium cacodylate, 0.2 mM EDTA; buffer C: 100 mM NaCl, 10 mM sodium cacodylate and 10 mM $MgCl_2$. Some data discussed below have been obtained in a previous investigation in the following two buffers: E5 and E10 contain 5 and 10 mM NaCl, respectively, in addition to the components of buffer E. All reagents were of analytical grade with the exception of cacodylic acid, which was obtained as crystalline grade from Sigma.

Electrooptical data were measured by a recently developed instrument, which is described in detail elsewhere [19]. The instrument is based on the cable discharge technique and produces pulses up to 40 kV for 200 ns with rise and decay times of a few ns. The limit time resolution of the optical detection unit also is a few ns. The required sample volume of 125 μl is filled into a cell with 5 mm optical pathlength and a distance of 5 mm between the Pt electrodes. The instrument is driven for automatic sampling via a transient recorder (Tektronix 7612D or 7912AD) by a personal computer with online control of the sample temperature and minimal exposure of the sample to ultraviolet irradiation by a computer-driven shutter.

The experimental data were transferred to the Gesellschaft für wissenschaftliche Datenverarbeitung mbH Göttingen for analysis of the decay curves. The decay time constants were usually evaluated by a fitting procedure designed by Provencher [21]. For comparison, two other independent fitting procedures [22,23] have been applied and provided the same results within an

accuracy limit of ±5% for fits with more than a single exponential. Moreover, results from independent experiments confirm that the accuracy of the time constants associated with the slow processes of two- and three-exponential fits is approx. ±5%. The accuracy of the time constants derived from mono-exponential fits is usually at ±1%, but is around ±2% for the short fragments with 41 and 43 bp.

3. Results

3.1. Measurements of dichroism decay curves

The dichroism decay curves were routinely measured at parallel orientation of polarized light and electric field vector. Controls showed that there were no effects at the magic angle orientation under the present experimental conditions. Thus, the electric field pulses did not induce any denaturation or conformation changes of the double helices. Furthermore, it was checked that the absorbance change at parallel and perpendicular orientation of light and field vector $\Delta A_{\parallel}$ and $\Delta A_{\perp}$ were consistent with $\Delta A_{\parallel} = -2\Delta A_{\perp}$. Thus, the observed effects are entirely due to field-induced alignment of DNA double helices. Usually 10 up to 20 pulse experiments were accumulated for a satisfactory signal-to-noise ratio. The dichroism decay curves measured for short DNA fragments up to 90 bp could be fitted by single exponentials to a high degree of high accuracy (cf. fig. 1), whereas the decay curves of fragments with 138, 166 and 179 bp clearly required two exponentials (cf. fig. 2). In the case of the fragment with 90 bp, the quality of the fits for experiments with high electric field pulses could be improved by admitting two exponentials. The decay curves measured for the fragment with 256 bp required three exponentials for optimal fitting.

Due to the rather high conductivity of the samples, electric field pulses always induced some increase of the temperature. The temperature jump was calibrated by measurements with a simple indicator system and proved to be consistent with expectation according to applied voltage, duration of the pulse, resistance and heat capacity of the

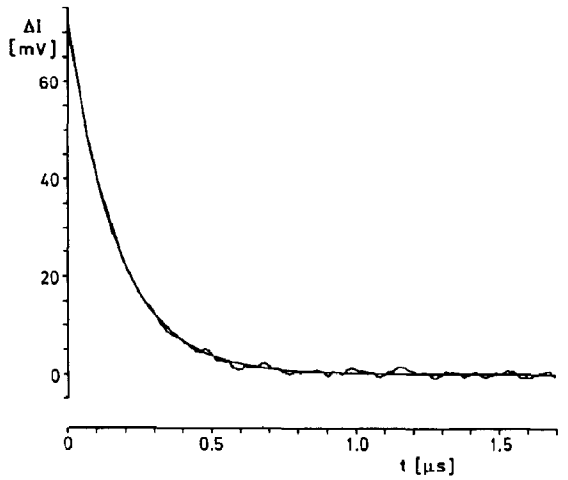

Fig. 1. Dichroism decay curve of a DNA restriction fragment with 43 bp in buffer C at 2°C (average of 20 shots with 60 kV/cm, recorded at 248 nm, 2.94 μM DNA helix, fitted exponential time constant $\tau = 169$ ns, after correction for temperature jump τ (2°C) = 174 ns).

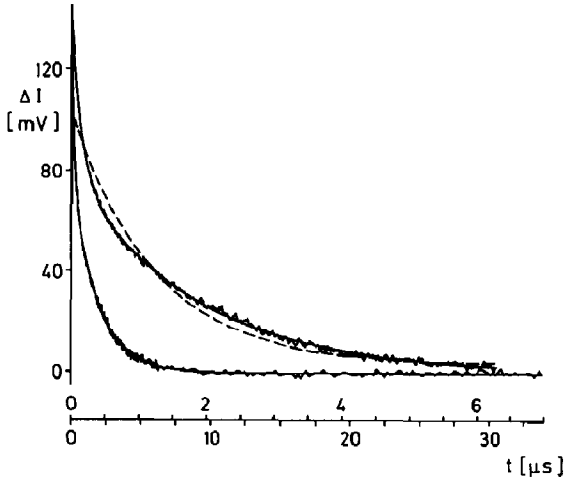

Fig. 2. Dichroism decay curve of a DNA restriction fragment with 138 bp in buffer C at 10°C, shown at two time scales. The continuous line, which can hardly be distinguished from the measured data, represents a least-squares fit with two time constants; the dashed line represents a least-squares 'fit' by a single exponential (average of 20 shots with 70 kV/cm recorded at 248 nm, 0.77 μM DNA helix, fitted time constants (values corrected to 10°C in brackets, cf. text) $\tau_1 = 121$ ms (126 ns), $\tau_2 = 1.83$ μs (1.91 μs) and amplitudes $A_1 = 68$ mV, $A_2 = 78$ mV). Note that the time constants given in the tables and in fig. 4 represent an average obtained from several experiments.

TABLE 1

Dichroism decay time constants (ns) observed for blunt-ended DNA restriction fragments in buffers of different ion composition (20 °C; estimated accuracy 43 bp: ±2%, 69 and 84 bp: ±1% and 179 bp: ±2.5%; the data for buffers E and M are from ref. 4)

Buffer	$[Na^+]$ (mM)	$[Mg^{2+}]$ (mM)	Chain length (bp)			
			43	69	84	179
E	2.4	–	102	317	525	3150
M	2.0	0.1	103	296	467	2770
A	101	–	97	269	418	2540
C	110	10	99	275	407	2440

sample. For the highest field pulses of 80 kV/cm the temperature jump was 1.4 °C (at a starting temperature of 2 °C in buffer C). All the measured time constants were corrected for the individual temperature jump effect to the initial temperature by the standard viscosity/temperature conversion factor. The magnitude of this correction was in the range up to 6%. After correction for the temperature jump effect the measured dichroism decay time constants proved to be independent of the electric field strength. The time constants were also reproducible in subsequent series of experiments on a given sample. Thus, any damage induced by the electric field pulses and the ultraviolet irradiation in the double helices, which might be accumulated after a series of pulses, do not affect the measured rotation time constants. Some of the corrected time constants are compiled in table 1 together with data obtained previously [4] at low salt concentrations.

Any interactions between DNA fragments, which might be favoured by the relatively high salt concentration used in the present investigation, would have a strong effect on the measured time constants. Measurements demonstrate, however (cf. fig. 3), that the dichroism decay time constants of blunt-ended fragments are not dependent on the DNA concentration. Thus, the time constants obtained for the blunt ended fragments are not affected by any intermolecular association and reflect unperturbed monomolecular rotational diffusion. In contrast to these results, measurements on fragments with short single-stranded complementary ends resulting from *Eco*RI digestion show a strong concentration dependence of their dichroism decay time constants, which appears to be due to association by base-pairing (unpublished results).

Because the electrooptical transients used for the present analysis have been generated by relatively short electric field pulses, it might be suspected that these pulses are not sufficient to induce electrooptical decay curves, which are representative of the complete spectrum of rotational diffusion time constants. Obviously, electrooptical amplitudes associated with slow diffusion processes will be reduced compared to those associated with fast processes, when short electric field pulse are used. Nevertheless the amplitudes associated with slow processes should be induced sufficiently up to a certain limit given by the rate of the rotational diffusion and its acceleration under electric field pulses. Because of this limit the present investigation was restricted to fragment lengths $n \leq 256$ bp. Another reason for the restriction to $n \leq 256$ bp is the fact that the number of relaxation processes increases with the chain length and thus the assignment of the processes including the slowest one is more difficult for long chains.

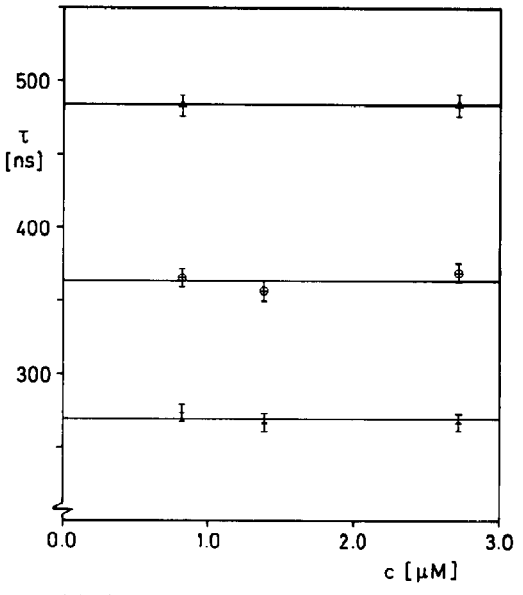

Fig. 3. Dichroism decay time constants of a DNA restriction fragment with 69 bp as a function of the helix concentration at 2(+), 10 (○) and 20 (Δ) °C (buffer A).

Test experiments performed with a standard pulse generator used at 'low' salt concentrations demonstrated that for chain lengths $n \leq 256$ bp the process with the slowest relaxation time constant remains unambiguously detectable also after short pulses, which do induce much less than the stationary level of the dichroism.

3.2. Evaluation of persistence lengths

The corrected 'slow' components of the dichroism decay curves represent the overall rotational diffusion of the DNA fragments. It is well known that these time constants are very strongly dependent on the effective hydrodynamic dimensions. The dependence of the dichroism decay time constants on the chain length provides accurate information on the persistence length. A standard model for the evaluation of the persistence length p from these experimental data has been given by Hearst [23]. According to his 'weakly bending rod' model the rotation diffusion coefficient is

$$D_h = \frac{kT}{\eta_0 \pi L^3}\left[3(L/b) - 7 + 4(b/a) + \lambda L\{2.25 \ln(L/b) - 6.66 + 2(b/a)\}\right]$$

where kT is the thermal energy, η_0, the solvent viscosity, L the contour length, b the distance between frictional elements, a the Stokes diameter of each element and $1/\lambda$ the Kuhn statistical segment length [24] corresponding to twice the persistence length p. The rotation diffusion coefficient is related to the rotation time constants τ_h by

$$\tau_h = \frac{1}{6D_h}$$

For the present evaluation it will be assumed that the double helices are, under the conditions of the measurements, in the standard B-helix conformation with a length increment of 3.4 Å per base-pair. This is justified by the correspondence of CD spectra with those of usual B-helices. A standard value of 50 Å has been used for the distance between frictional elements [23]. The two remaining parameters — the persistence length and the Stokes diameter — were evaluated by least-squares fitting of the experimental rotation time constants.

More recently, Hagerman and Zimm [25] developed a model for the rotational diffusion of worm-like chains on the basis of Monte Carlo calculations. Their results are given as a correction factor

$$R = (1.0120 - 0.24813x + 0.033703x^2 - 0.0019177x^3) \cdot (1 - 0.06469x + 0.01153x^2 - 0.0009893x^3)$$

to the transverse rotational diffusion coefficient of a rigid cylinder presented by Broersma [26]

$$D_b = \left(3kT/\pi\eta_0 L^3\right)\left\{\ln(L/r) - 1.57 + 7\left[1/\ln(L/r) - 0.28\right]^2\right\}$$

x is the ratio L/p and r the radius of the cylinder. The rotational diffusion time constant of a wormlike chain according to Hagerman and Zimm is given by $\tau_b = R/6D_b$. The free parameters, persistence length p and the radius r, have been evaluated by least-squares fitting of the experimental data.

The dichroism decay time constants measured as a function of the chain length can be represented by both models to a high degree of accuracy. However, the parameters resulting for the persistence length and the hydrodynamic radius of the DNA double helix are consistently different. While the Hearst model indicates t-values ($\sim$ 12.5 Å) which are in the range expected according to crystal structures of double helices [27], the r values resulting from the Hagerman-Zimm model ($\sim$ 9 Å) are lower than expected. The p-values determined by the Hearst model are clearly lower than those obtained by the Hagerman-Zimm model. Hagerman and Zimm avoided some assumptions inherent in the Hearst model. However, they used a reference formula for rigid rods, which has been revised since then.

For a reliable determination of the persistence length and of the hydrodynamic radius, the evaluation of the experimental data should be based on one of the revised expressions for the rotational diffusion of rigid rods. Thus, the present experimental data have been evaluated also

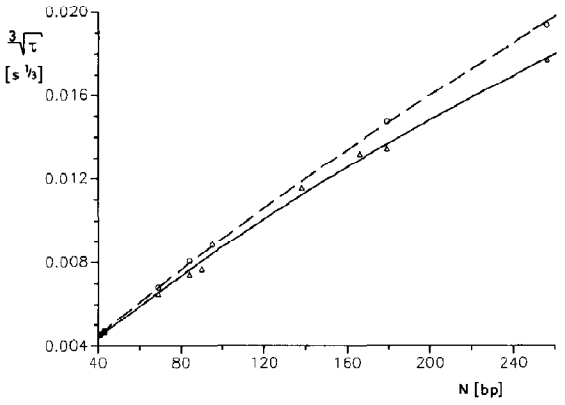

Fig. 4. Cubic root of the dichroism decay time constants (Δ) as a function of the DNA chain length in units of base-pairs at 20 °C in buffer C. The continuous line represents a fit by the combined model with a persistence length $p_t = 440$ Å and a hydrodynamic radius $r_t = 12.3$ Å. For comparison the results obtained in the low salt buffer E [4] are represented by circles and the corresponding fit with the combined model by the dashed line.

on the basis of a 'combined' model using the rotational diffusion coefficient given for rigid rods by Tirado and Garcia de la Torre [28,29]

$$D_t = \left(3kT/\pi\eta_0 L^3\right) \times \left\{\ln(q) - 0.662 + 0.917/q - 0.050/q^2\right\}$$

where $q = L/(2r)$. The correction factors derived by Hagerman and Zimm [25] are applied for the calculation of rotational time constants according to $\tau_t = R/6D_t$. An example of a least-squares fit is given in fig. 4. For an unequivocal assignment of the parameters, the indices h, b and t are used to label persistence lengths p and hydrodynamic radii r obtained from the models of Hearst, Hagerman and Zimm with the Broersma equation, and Hagerman and Zimm with the Tirado and Garcia de la Torre equation, respectively.

As shown in table 2 the persistence lengths determined according to the combined model are in the range $p_t = 360$–440 Å and the hydrodynamic radius r_t is around 12.5 Å. Within experimental accuracy the p-values at these high ionic strengths of $I \approx 100$ mM are not dependent upon details of the buffer composition; addition of 10 mM Mg^{2+} does not induce any change of the p-value , within experimental accuracy. However, a decrease of the temperature leads to a clearly detectable decrease of the persistence length.

3.3. Bending time constants

In addition to the overall rotation time constants, the dichroism decay curves provide information on the DNA bending dynamics, which is reflected by the fast components of the dichroism decay curves measured for fragments with chain lengths above 100 bp. The arguments for this assignment have been discussed in previous publications [4,22,30] and, thus, are not repeated here. In the present investigation, the pulses are not sufficiently long to induce a stationary degree of

TABLE 2

Persistence lengths p and hydrodynamic radius r (in Å) from dichroism decay time constants evaluated by different hydrodynamic models (cf. text); estimated accuracy r: ±0.2 Å, P: ±5%; the parameters given for buffer C have been evaluated from experimental data for the complete collection of nine restriction fragments (cf. section 2), whereas the parameters for buffer A (B) are based on measurements for the fragments with 43, 69, 84, 179 and 256 bp (43, 69, 84 and 179 bp)

Buffer	$[Na^+]$ (mM)	$[Mg^{2+}]$ (mM)	Temp. (°C)	Hearst		Hagerman and Zimm		Tirado and Garcia de la Torre/ Hagerman and Zimm	
				p_h	r_h	p_b	r_b	p_t	r_t
C	110	10	20	304	12.5	490	8.75	440	12.3
C	110	10	10	272	12.6	444	8.91	403	12.5
C	110	10	2	251	12.6	412	9.17	377	12.9
A	101	–	20	293	12.3	480	8.35	437	11.6
A	101	–	10	278	12.4	457	8.54	418	11.9
A	101	–	2	231	12.4	385	8.83	356	12.3
B	101	–	20	318	12.4	512	8.40	455	11.8

TABLE 3

Bending time constants (in ns) of DNA double helices as a function of the chain length and the temperature; numbers in parenthesis give the bending time constants relative to the overall rotational diffusion time constants in % (from dichroism decay curves measured in 100 mM NaCl, 10 mM $MgCl_2$, 10 mM sodium cacodylate pH 7; estimated accuracy ± 10%)

Chain length (bp)	Temperature (°C)		
	20	10	2
90	–	58	74
	–	(9.2)	(8.6)
138	112	134	169
	(7.3)	(6.8)	(7.0)
166	196	241	313
	(8.5)	(8.4)	(9.0)
179	246	279	349
	(10.0)	(9.0)	(8.8)

the orientation and bending equilibrium in the presence of the electric field. Thus, bending amplitudes cannot be evaluated quantitatively. As shown by the example in fig. 2 the amplitude of the fast component is relatively large due to the fact that (partial) stretching is induced more quickly than alignment along the long axis. Nevertheless, the time constants should not be affected by this technical problem. Bending time constants measured for various chain lengths are compiled in table 3. Virtually all these bending time constants are between 7 and 9% of the respective overall rotational diffusion time constant.

4. Discussion

A direct comparison of dichroism decay time constants measured in different buffer solutions (cf. table 1) demonstrates that the effective hydrodynamic dimensions of DNA double helices are very strongly dependent on the ion concentration. An increase of the monovalent salt concentration from approx. 2 mM to approx. 100 mM leads to a decrease of the dichroism decay time constant by 20% for a fragment with 84 bp. Obviously this change is due to a reduction of electrostatic repulsion between phosphate charges. At a low monovalent salt concentration the electrostatic repulsion can be partly shielded by addition of 0.1 mM $MgCl_2$; at a high monovalent ion concentration addition of even 10 mM $MgCl_2$ does not induce any clearly detectable change of the time constants. Thus, Mg^{2+} does not have any specific effect on the global structure of DNA double helices, but simply contributes to the general shielding of phosphate repulsion.

The conclusions derived qualitatively by direct inspection of the experimental time constants are confirmed by the analysis using hydrodynamic models. Although the absolute hydrodynamic parameters derived form the various models are quite different, all models show a clear decrease of the persistence length, when the monovalent salt concentration is increased from the range around 2 mM to physiological conditions with ionic strengths around 100 mM.

4.1. Hydrodynamic models

Before the new experimental results are compared with those obtained in previous investigations by various laboratories, some comments are necessary regarding the hydrodynamic models used for evaluation. Although the results derived by different models can be quite different, this difference has been ignored almost completely. Apparently, this is partly due to the fact that three independent early electrooptical investigations of the global DNA structure provided the same value of the persistence length (~ 500 Å), although the Hearst model was used for two of the evaluations [1,3] and the Hagerman-Zimm model for the third one [2]. This has led to the impression that the results derived by the different models are almost equivalent. Hagerman [31], for example, comments "that the weakly bending rod model of Hearst... leads to underestimation" of the persistence length p, but he concluded in the same paper that "the choice of the model is almost certainly not the source" of a particularly low p value [4] found in the presence of Mg^{2+}. In this special case the choice of the model turns out to be the main source for diverging conclusions.

For a direct demonstration of the model difference it is instructive to fit rotation time constants, which are calculated according to the Hearst model, by the Hagerman-Zimm model.

Using $p_h = 350$ Å and $r_h = 13$ Å together with a frictional distance of 50 Å for the Hearst model in the range of chain lengths from 40 to 500 bp provides a virtually perfect fit by the Hagerman-Zimm model with $p_b = 570$ Å and $r_h = 9.5$ Å. Thus, the difference in the model parameters is rather large and results may be compared only when derived from the same model. The model of Hagerman and Zimm, based on Monte Carlo simulations, avoids some assumptions inherent in the earlier approach presented by Hearst. However, Hagerman and Zimm used an expression for the rotational diffusion of rigid rods given by Broersma [26], which has been revised since then by Tirado and Garcia de Torre [28,29] and also by Broersma [32] himself. Thus, the most reliable model currently available should result from a combination of one of the more recent equations for the rotational diffusion of rigid rods with the correction factors derived by Hagerman and Zimm. The equation given by Tirado and Garcia de la Torre was chosen for this purpose.

For a comparison of persistence lengths obtained under different conditions, the experimental data determined previously in this laboratory have been evaluated both by the Hagerman-Zimm model and by the combined model (cf. table 4). At a monovalent salt concentration of 2 mM the persistence length p_t is 872 Å (±5%) corresponding to about 250 bp. An increase of the salt concentration to 7 mM and to 12 mM leads to a decrease of p_t to 721 and 559 Å (±5%), respectively. Addition of Mg^{2+} induces a further decrease of p_t to 504 Å (±5%). The present measurements demonstrate that the decrease of the persistence length continues, when the salt concentration is increased to 100 mM.

4.2. Comparison with other electrooptical data

First, these results obtained by electrooptical measurements should be compared with data obtained by the same method from other laboratories. Hagerman [2] has reported persistence lengths measured at low salt concentrations, which are similar but not identical with those given in table 4. He concluded that there is "no strong ionic strength dependence of the persistence length for ionic strengths above 1 mM". Hagerman reports a persistence length $p_b = 500$ Å already at monovalent salt concentrations around 2 mM, which is not consistent with the data given in table 4. Some of this difference may be due to the fact that Hagerman apparently did not routinely add as much EDTA for his measurements in monovalent salt solutions as was present during the corresponding measurements used for the data compiled in table 4. Small contaminations of multivalent ions, which are difficult to avoid in electrooptical experiments due to the contact of solutions with metal electrodes, have a particularly strong effect on rotational diffusion coefficients at low salt concentrations and thus should be trapped by a sufficiently high EDTA level. A very clear difference is found with respect to the hydrodynamic radius of the double helix: Hagerman [2] reports

TABLE 4

Persistence lengths and hydrodynamic radii (in Å at 20°C) at different ion concentrations according to different hydrodynamic models; the data used for the parameters in buffers E, E5, E10 and M are from ref. 4; estimated accuracy r: ±0.2 Å, p: ±5%

Buffer	$[Na^+]$ (mM)	$[Mg^{2+}]$ (mM)	Hearst		Hagerman and Zimm		Tirado and Garcia de la Torre/ Hagerman and Zimm	
			p_h	r_h	p_b	r_b	p_t	r_t
E	2.4	–	703	13.2	1020	9.4	872	13.0
E5	6.4	–	600	12.1	848	9.5	721	13.3
E10	12	–	577	13.3	670	10.0	559	14.3
M	2	0.1	354	12.9	557	9.3	504	13.0
A	101	–	292	12.3	480	9.3	437	11.6
C	110	10	304	12.5	490	8.8	440	12.3

values around $r_b = 13$ Å, whereas the data obtained in this laboratory evaluated by the Hagerman-Zimm model provide values $r_b = 9$–10 Å, depending on the ion concentration. Probably part of this difference results from the fact that the set of experimental data used for the parameters given in table 4 included data for relatively short fragments measured at a particularly high time resolution.

Another set of dichroism decay time constants has been reported by Elias and Eden [1], who analyzed their data by the Hearst model with a rise per base-pair of 3.15 Å. An evaluation of their data by the Hagerman-Zimm model with a rise per base-pair of 3.4 Å provides a persistence length $p_b \sim 600$ Å and a helix radius $r_b \sim 13$ Å. Elias and Eden collected their data at 4° C (1 mM Na^+, without EDTA) which may be a reason for some difference with respect to the other low salt data measured at 20° C.

It may be concluded that the electrooptical data collected in different laboratories at low salt concentrations are not equivalent, but nevertheless differences remain limited. At salt concentrations around 1 mM the persistence length clearly decreases with increasing salt concentrations. From the data obtained in the low salt range it was not really possible to extrapolate the persistence length at physiological ion concentration. The present measurements demonstrate that the decrease of the persistence length with increasing salt continues up to at least 100 mM Na^+.

4.3. Ionic strength dependence

As shown in fig. 5, the persistence lengths measured in buffers containing Na^+ (without Mg^{2+}) can be represented within experimental accuracy as a linear function of the reciprocal square root of the ionic strength. This dependence is qualitatively consistent with model calculations presented by Le Bret [33] and by Fixman [34] on the basis of numerical solutions of the Poisson–Boltzmann equation: the electrostatic contribution to the persistence length calculated for salt concentrations from 1 mM to 1 M can also be given as a linear function of the reciprocal square root of the ionic

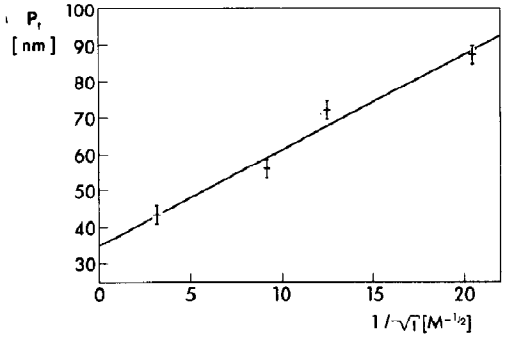

fig. 5. Persistence length p_t (in nm) measured in buffers containing Na^+ as cations (without Mg^{2+}) as a function of the reciprocal square root of the ionic strength I.

strength *. However, the slope derived from the experimental data is about a factor of 2 higher than that expected according to the calculations. The difference may be due to some approximations and/or a special choice of parameters used in the calculations, but may also reflect some change of the DNA structure induced by changes of the salt concentration.

4.4. Recent results obtained by other techniques

The persistence length has been measured by other authors and techniques, which cannot be discussed in depth because of space limitations. Most of the measurements have been on samples, which cannot be regarded as well defined accord-

* The linear dependence of the persistence length on the reciprocal square root of the salt concentration was found accidentally upon data inspection and proved to represent the data more accurately than other simple functions. Subsequently, it was found during a check of the literature that both the Le Bret and the Fixman calculations predict the relationship resulting from the present experiments. Thus, the special dependence has not been 'imposed' on the data because of the theoretical prediction. After submission of this manuscript a comment was given by the editor that the same dependence has been used before the Tricot [35] for the description of data obtained for some synthetic polyelectrolytes. In a comment received after revision it was pointed out that a p versus $1/\sqrt{I}$ plot has been used for the case of DNA already in a short report given by Geller [40]; the data shown by Geller are for sonicated DNA and suggest a non-linear p versus $1/\sqrt{I}$ dependence.

ing to the present state of the art. A detailed investigation of a well defined plasmid DNA has been presented by Eisenberg and co-workers [6–8]. Based on measurements of light scattering, they arrived at a persistence length of 450 Å at 0.2 M Na^+ and at a limiting value of approx. 320 Å at 1 M Na^+. It has been argued that their values are affected by a systematic error due to excluded volume effects. The present results obtained in a range of chain lengths, where excluded volume does not affect results at all, indicate that any errors in the evaluation of Eisenberg et al. are probably not essential (for a discussion of data collected up to 1978 from the viewpoint of polyelectrolyte theory, cf. ref. 36).

Finally, it should be mentioned that experiments on DNA circularization [14,15] catalysed by a ligase enzyme have been used for the evaluation of persistence lengths. The value of about 500 Å resulting from this 'biochemical' technique is larger than that obtained by 'physical' techniques using electrooptics and light scattering, but remains in the range of variation to be expected due to sequence dependent modulation of DNA structure.

The hydrodynamic radius r evaluated from the present measurements appears to be in contrast with a recent investigation of Eimer et al. [37], who reported an r value of 10.2 ± 0.5 Å derived from measurements of dynamic light scattering on the basis of the Tirado and Garcia de la Torre model. However, their data were collected for short fragments with alternating GC base-pairs, whereas the present results are for mixed GC/AT sequences. Thus, it may be that the hydrodynamic radius depends on the nucleotide sequence. This possibility is under further investigation.

4.5. Sequence-dependent variation of DNA structure

The present results show a rather large variation of 'individual' persistence lengths derived from the rotational diffusion time constants of single DNA restriction fragments (table 5). Due to this variation it is almost impossible to define a standard DNA persistence length. The strong sequence dependence of the DNA structure is also demonstrated by different temperature dependences of 'individual' persistence lengths. While the 'average' persistence length decreases with decreasing temperature, some fragments show an increase of their 'individual' persistence length with decreasing temperature. Thus, results obtained on average persistence lengths will depend on the DNA fragments selected for investigation. The opposite temperature dependence may be easily explained in terms of current models on DNA structure. A decrease of the persistence length with increasing temperature would be consistent with the common view that the double helix is mainly stabilized by stacking interactions. Because the free energy of base stacking increases with decreasing temperature, it would be expected that the stiffness increases at low temperatures. The opposite temperature dependence may be due to sequence-directed DNA curvature, which is known to be favoured at low temperatures. The experimental persistence length is affected both by thermal bending and by sequence-directed curvature [38,39]. It is rather difficult to distinguish between these effects on the basis of the available experimental data. Another contribution to variations of the global DNA structure may come from a sequence dependence of the helix rise per base-pair. All the evaluations given above were based on the assumption of a standard 3.4 Å rise per base pair. Further measurements is an extended range of temperatures will be necessary for an

TABLE 5

Individual persistence lengths (in Å) of some DNA restriction fragments according to combined model (Tirado and Garcia de la Torre/Hagerman and Zimm) evaluated with a constant hydrodynamic radius of 12.5 Å (dichroism decay time constants in ns are given in brackets; buffer C; 20 °C; estimated accuracy ±5%). The radius 12.5 Å represents the average value found from fitting of the complete data sets measured in buffer C (cf. table 3)

Temperature (°C)	Chain length (bp)		
	166	179	256
2	340	315	460
	(3490)	(3970)	(10300)
10	420	340	435
	(2880)	(3110)	(7640)
20	540	385	425
	(2310)	(2440)	(5580)

unequivocal assignment of these different contributions to the global structure of DNA double helices.

Acknowledgements

The author is indebted to B. Krahmer and J. Wawrzinek for technical assistance in the electrooptical measurements and the preparation of the DNA fragments.

References

1 J.G. Elias and D. Eden, Macromolecules 14 (1981) 410.
2 P.J. Hagerman, Biopolymers 20 (1981) 1503.
3 S. Diekmann, W. Hillen, B. Morgeneyer, R.D. Wells and D. Porschke, Biophys. Chem. 15 (1982) 263.
4 D. Porschke, J. Biomol. Struct. Dyn. 4 (1986) 373.
5 R.J. Lewis, R. Pecora and D. Eden, Macromolecules 19 (1986) 134.
6 N. Borochov and H. Eisenberg, Biopolymers 20 (1981) 2671.
7 N. Borochov and H. Eisenberg, Biopolymers 23 (1984) 1757.
8 H. Eisenberg, Acc. Chem. Res. 20 (1987) 276.
9 K.L. Cairney and R.E. Harrington, Biopolymers 21 (1982) 293.
10 R.E. Harrington, Biopolymers 17 (1978) 919.
11 M. Mandel and J. Schouten, Macromolecules 13 (1980) 1247.
12 G. Maret and G. Weill, Biopolymers 22 (1983) 2727.
13 C. Frontali, E. Dore, A. Ferrauto, E. Gratton, A. Bettini, M.R. Pozzan and E. Valdevit, Biopolymers 18 (1979) 1353.
14 D. Shore, J. Langowski and R. Baldwin, Proc. Natl. Acad. Sci. U.S.A. 78 (1981) 4833.
15 W.H. Taylor and P.J. Hagerman, J. Mol. Biol. 212 (1990) 363.
16 J.M. Schurr and K.S. Schmitz, Ann. Rev. Phys. Chem. 37 (1986) 271.
17 C.T. O'Konski, Molecular electrooptics, vol. I. Theory and methods (1976); vol. II. Applications to biopolymers (Dekker, New York, 1978).
18 E. Fredericq and C. Houssier, Electric dichroism and electric birefringence (Clarendon, Oxford, 1973).
19 D. Porschke and A. Obst, Rev. Sci. Instrum. (1990) in the press.
20 M. Colpan and D. Riesner, J. Chromatogr. 296 (1984) 339.
21 S.W. Provencher, Biophys. J. 16 (1976) 27.
22 D. Porschke and M. Jung, J. Biomol. Struct. Dyn. 2 (1985) 1173.
23 J.E. Hearst, J. Chem. Phys. 38 (1963) 1062.
24 H. Kuhn, W. Kuhn and A. Silberberg, J. Polym. Sci. 14 (1953) 193.
25 P.J. Hagerman and B.H. Zimm, Biopolymers 20 (1981) 1481.
26 S. Broersma, J. Chem. Phys. 32 (1960) 1626.
27 W. Saenger, Principles of nucleic acid structure (Springer, Berlin (1984)).
28 M.M. Tirado and J. Garcia de la Torre, J. Chem. Phys. 73 (1980) 1986.
29 M.M. Tirado, C.L. Martinez and J.Garcia de la Torre, J. Chem. Phys. 81 (1984) 2047.
30 D. Porschke, Biopolymers 28 (1989) 1383.
31 P.J. Hagerman, Annu. Rev. Biophys. Chem. 17 (1988) 265.
32 S. Broersma, J. Chem. Phys. 74 (1981) 6989.
33 M. Le Bret, C. R. Acad. Sci. Paris 292 (1981) 291.
34 M. Fixman, J. Chem. Phys. 76 (1982) 6346.
35 M. Tricot, Macromolecules 17 (1984) 1698.
36 G.S. Manning, Q. Rev. Biophys. 11 (1978) 179.
37 W. Eimer, J.R. Williamson, S.G. Boxer and R. Pecora, Biochemistry 29 (1990) 799.
38 K.E. Reinert, Biophys. Chem. 13 (1981) 1.
39 E.N. Trifonov, R.K.Z. Tan and S.C. Harvey, in: DNA bending and curvature, eds W.K. Olson, M.H. Sarma, R.H. Sarma and M. Sundaralingam (Adenine Press, New York, 1987) p. 243.
40 K. Geller, Studia Biophysica 87 (1982) 231.